

Geologic Hydrogen Exploration by Joint Inversion and Integrated Geological Interpretation

Yawei Su*, Sihong Wu, Jiajia Sun, Xuqing Wu, Yueqin Huang, and Jiefu Chen, University of Houston;
Ligang Lu, Shell Global Solutions; Xiaolong Wei, Stanford University; Rodolfo Christiansen, Leibniz Institute for Applied Geophysics.

Introduction

Hydrogen (H_2) is a highly promising clean energy source for the global transition toward renewable and cleaner energy. However, its early applications primarily positioned it as an energy carrier rather than a primary energy source. Recent attention has shifted toward geologic hydrogen ("Gold H_2 ") as an energy source, which naturally occurs and accumulates in the subsurface resulting from a range of natural processes, and the cost for exploiting geologic hydrogen is estimated to be 2 to 10 times smaller than the cost of manufactured hydrogen [1].

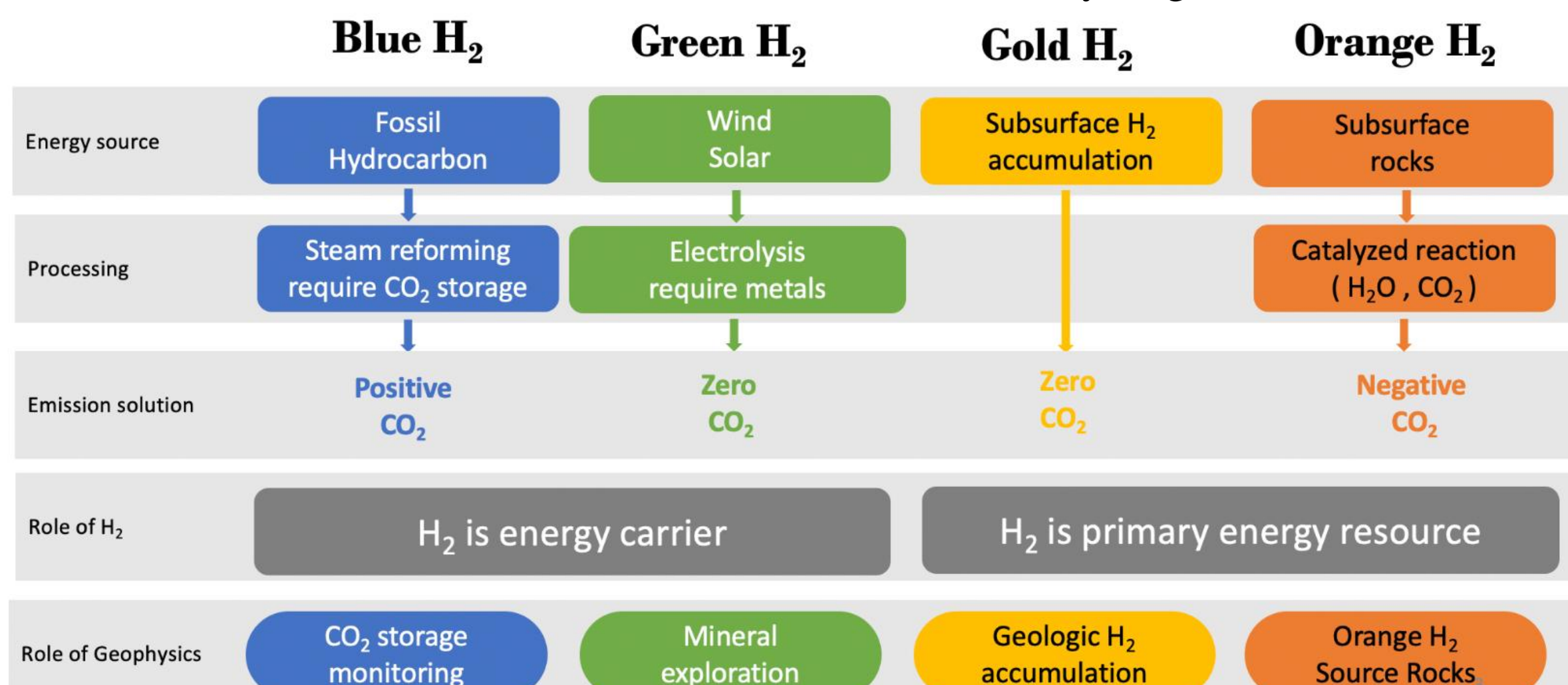


Figure 1. Color representation of different H_2 in energy transition. [2]

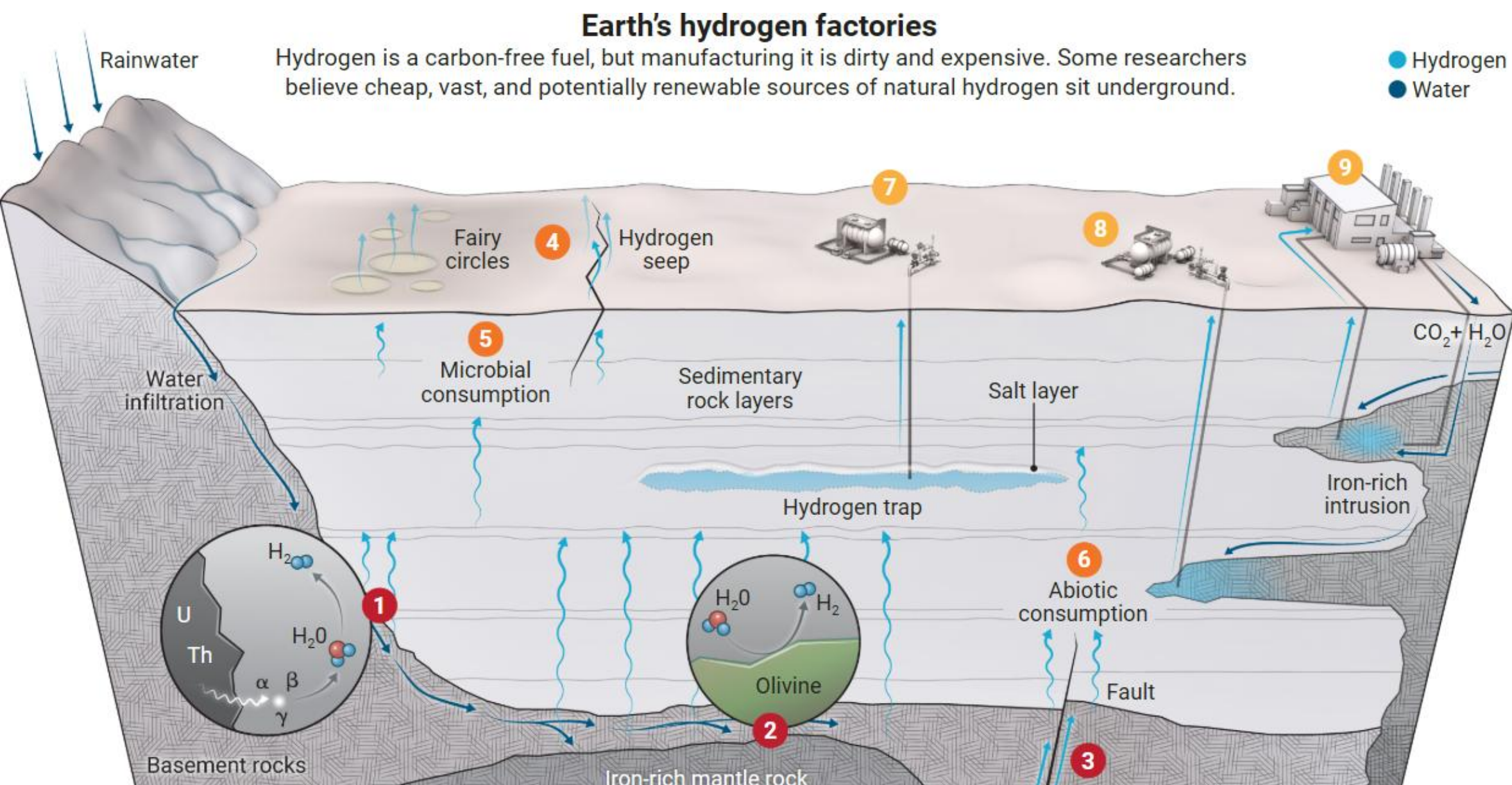


Figure 2. The schematic of generation and loss mechanisms and extraction method for geologic hydrogen.[3]

Serpentization is one of the well-studied generation mechanisms for geologic hydrogen, where iron-rich minerals, e.g., olivine in peridotite, are oxidized by water into serpentinite and produce hydrogen at high temperature (210~300 °C) [4]. This reaction will lower the density and increase the magnetic susceptibility of the target structure compared with the source rock (ultramafic rocks).



Compared with hydrocarbon in fossil fuel, hydrogen is generated much faster in the subsurface, and it is also highly reactive and diffusive, so the hydrogen reservoir should have a higher possibility to be found near its source [2]. As a result, serpentinite could be an indicator of the area where geologic hydrogen is likely to exist.

Methodology

The goal of our study is to develop an integrated workflow that combines multiple types of geophysical measurements and geological knowledge to identify favorable geological units for natural hydrogen accumulation. Our workflow consists of two main components: **joint inversion** and **geology differentiation**, as Figure 4 shows.

To locate the serpentinite and better estimate its distribution, we performed a **3D sparse joint inversion** using isostatic gravity anomaly and airborne total field magnetic anomaly data released by USGS. L1 norm is applied to the smallness regularization term to promote sparsity in the inverted model. The cross-gradient term enforces structural similarity between the models.

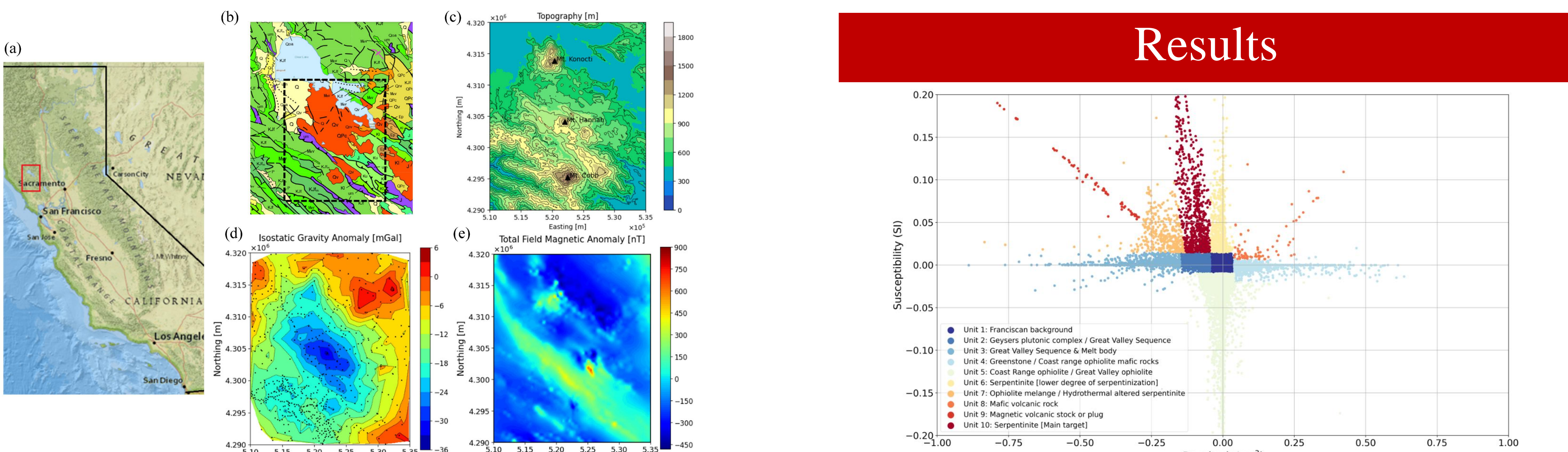


Figure 3. (a) The location of our area of interest (AOI) in California. (b) The surface geology map of our area of interest [5]. The purple unit represents the serpentized ophiolite, the dashed black box refers to the inversion core zone. (c) The topography map of our AOI. (d)(e) Visualized gravity and aeromagnetic data. The black dots in the gravity data map refer to the gravity measurement stations.

Table I. The density and magnetic susceptibility properties of local rocks. [6][7]

Rock type	Density (g/cm ³)	Susceptibility (SI)
Franciscan background	2.67 (0)	0
Geysers plutonic complex	2.52 – 2.62 (-0.15 – -0.05)	0
Great Valley sequence	2.52 – 2.67 (-0.15 – 0)	0
Greenstone*	2.70 – 3.14 (0.03 – 0.47)	0+
Coast Range ophiolite mafic rocks*	2.77 (0.1)	0+
Coast Range ophiolite	2.67 (0)	0.031**
Great Valley ophiolite	2.67 (0)	0.031**
Detrital serpentinite	2.57 (-0.1)	0.013 – 0.050
Mafic volcanic rock	2.77 – 2.87 (0.1 – 0.2)	0 – 0.026
Quaternary Clear Lake volcanics	2.47 – 2.67 (-0.2 – 0)	0.013 – 0.126
Serpentinite***	2.57 – 2.75 (-0.1 – 0.08)	0.031
Ophiolite mélange	2.47 – 2.77 (-0.2 – 0.1)	0 – 0.031

* Coast Range ophiolite mafic rocks and greenstone samples in this region are often magnetically dead.

** Could be lower down to 0.013 SI or larger up to 0.050 SI in some region. [6]

*** Higher density reflects incorporation of basalt and gabbro blocks. [6]

For **geology differentiation**, we firstly collected the density and magnetic susceptibility properties of the local rock types. Then, we summarized the density-susceptibility cross-plot derived from the 3D inverted model, where each scatter point represents one cell in the subsurface model with certain density contrast and magnetic susceptibility value compared with the background rock. According to Table 1, we initially segmented the cross-plot into one background unit and several other non-overlapping units. Then, starting from the background unit, we visualized each unit in form of its 3D spatial distribution model and 2D slices and compared it with corresponding anomalies in the inverted model to assess spatial consistency. After adjusting the segmentation on the cross-plot, each classified unit is assigned a geological interpretation considering both its physical properties and prior measurements and analysis, and **the final output is a 3D quasi-geology model** showing the spatial distribution of all geological units, as Figure 6 and 7 shows.

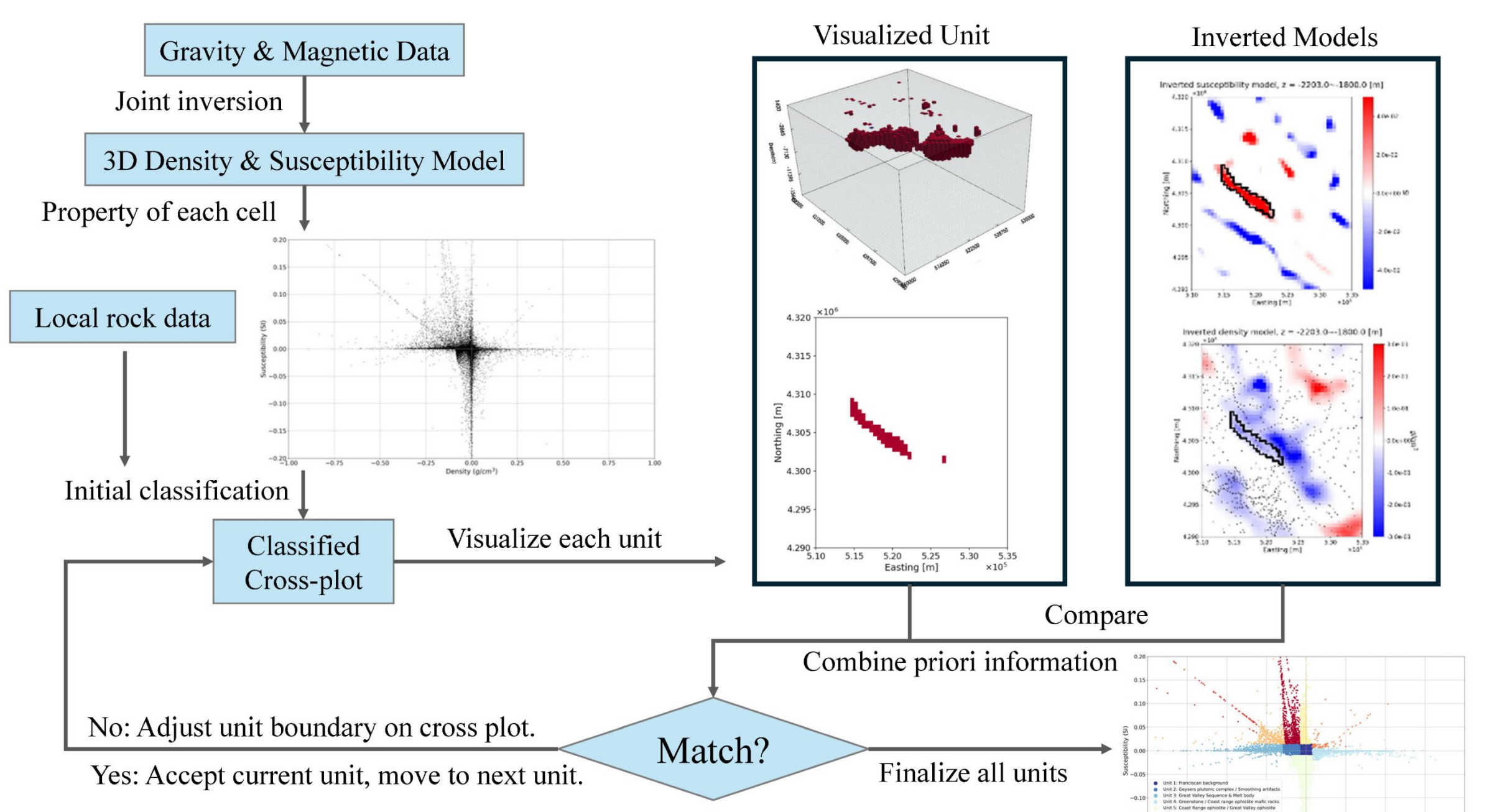


Figure 4. The schematic of the proposed workflow, illustrating geology differentiation process in detail.

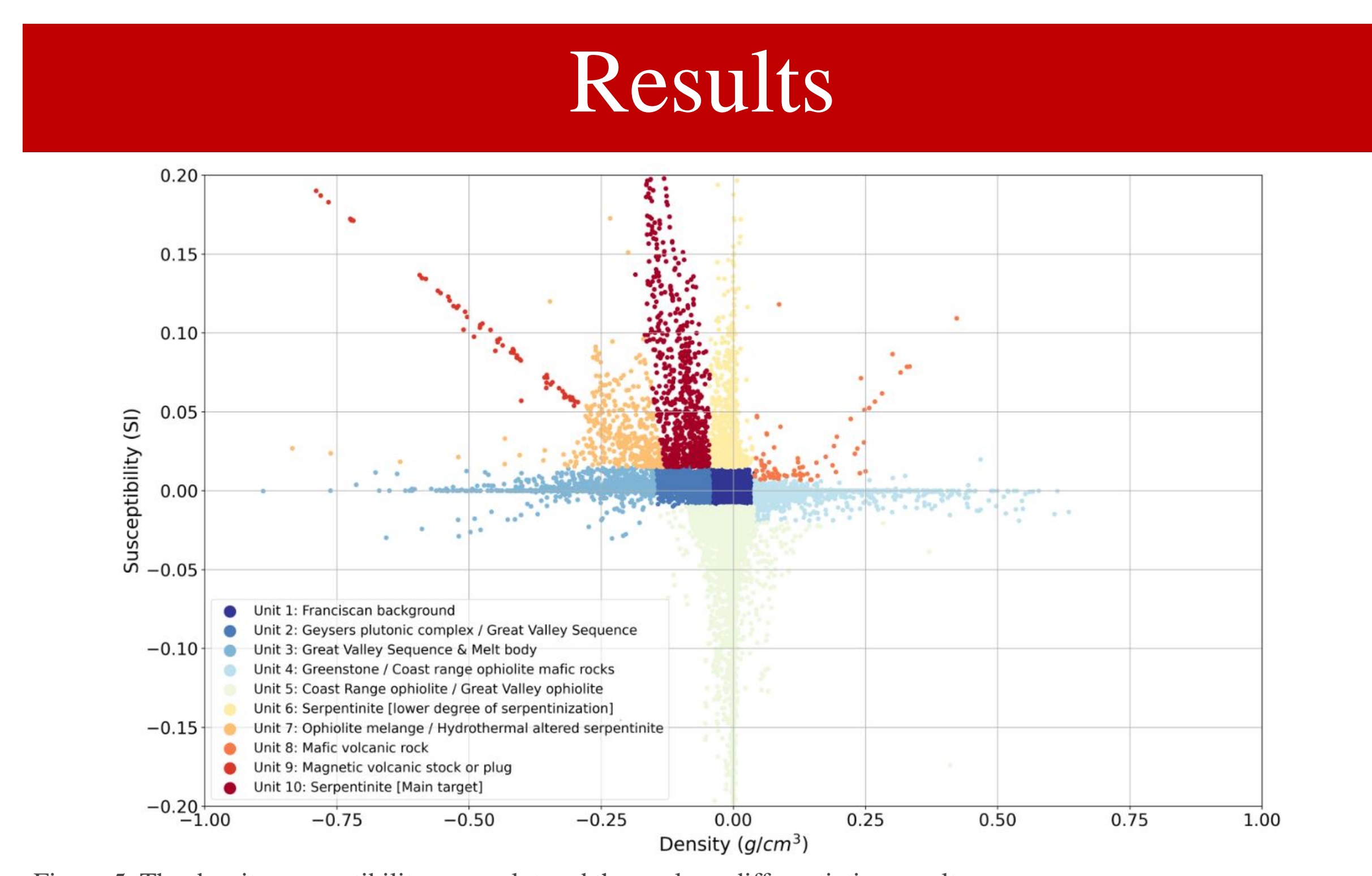


Figure 5. The density-susceptibility cross plot and the geology differentiation result.

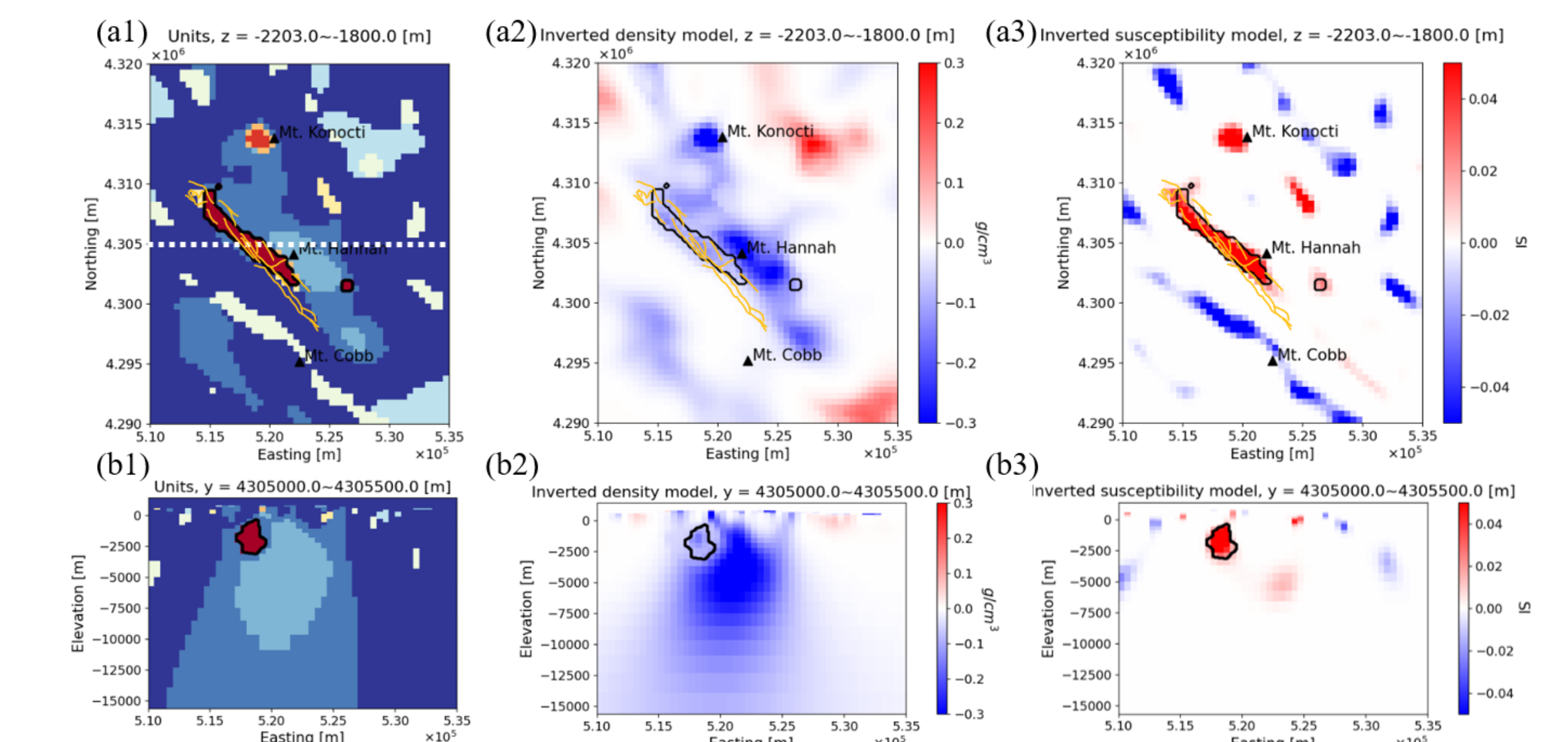


Figure 6. Geology differentiation result and inverted model for the primary serpentinite target in Unit 10. (a) The depth slices at 2 km depth and (b) vertical slices along the white dashed line for Unit 10. Column (1) shows the quasi-geology model, column (2) shows the inverted density models, and column (3) shows the inverted magnetic susceptibility models. Black contours outline the structure of Unit 10. The yellow stripes mark out a part of Collayone faults.

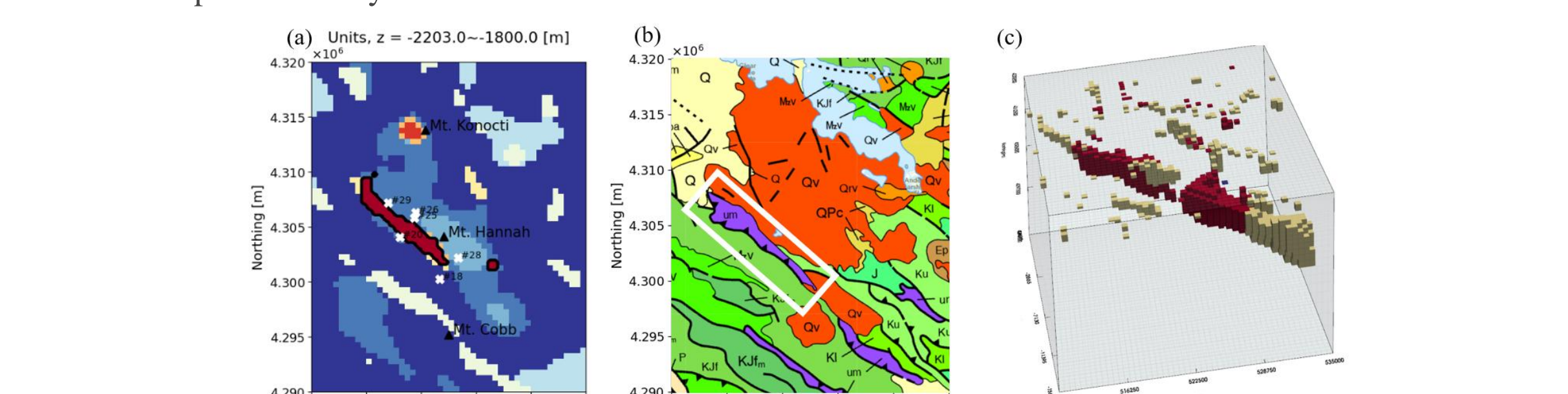


Figure 7. (a) The quasi-geology model slice at 2 km depth. The white crosses refer to the location of geothermal wells near the main serpentinite target. [8] (b) The surface geology map with the white box marks the outcropped serpentinite that is consistent with the main target. (c) Serpentinite Unit 10 (red) and Unit 6 (Yellow) in 3D quasi-geology model.

Conclusion

This study established a workflow that integrates gravity and airborne magnetic data to reconstruct 3D subsurface structures and employs geology differentiation to identify the serpentinite targets, thus indicates the possible searching area for geologic hydrogen. This workflow can be readily applied to other areas of interest, offering a cost-effective approach to geological hydrogen exploration without the need for drilling boreholes. For future work, we plan to combine machine learning approaches with our workflow to enhance the efficiency and accuracy.

References

- [1] Prinzhofen, A., Cissé, C.S.T. and Diallo, A.B., 2018. Discovery of a large accumulation of natural hydrogen in Bourakebougou (Mali). International Journal of Hydrogen Energy, 43(42), pp.19315–19326.
- [2] Zhang, M. and Li, Y., 2024. The role of geophysics in geologic hydrogen resources. Journal of Geophysics and Engineering, p.gxae056.
- [3] Han, E., Hidden hydrogen. Science 2023; 375 : Issue 6633, 630–6363. <https://www.science.org/content/article/hidden-hydrogen-earth-may-hold-vast-stores-renewable-carbon-free-fuel> (last accessed on April 22, 2024)
- [4] Zgonik, V., 2020. The occurrence and geoscience of natural hydrogen: A comprehensive review. Earth-Science Reviews, 203, p.103140.
- [5] Jennings, C.W., Gutierrez, C., Bryant, W., Sacedo, G. and Wills, C., 2010. Geologic Map of California: California Geological Survey Geologic Data Map 2, scale 1: 750,000. California Geological Survey, Sacramento, CA, US.
- [6] Langenheim, V.E., McLaughlin, R.J. and Melosh, B.L., 2024. Integrated geologic and geophysical modeling across the Bartlett Springs fault zone, northern California (USA): Implications for fault creep and regional structure. Geosphere, 20(1), pp.129–151.
- [7] Mitchell, M.A., Peacock, J.R. and Burgess, S.D., 2023. Imaging the magmatic plumbing of the Clear Lake Volcanic Field using 3-D gravity inversions. Journal of Volcanology and Geothermal Research, 435, p.107758.
- [8] Stamic, J.A., Goff, F. and Wohletz, K., 2001. Thermal modeling of the Clear Lake magnetic-hydrothermal system, California, USA. Geothermics, 30(2-3), pp.349–390.